

Investigation of the neuroprotective effects of a novel synthetic compound via the mitochondrial pathway

DI WANG^{1-3*}, SHUANG HU^{2*}, JUNRONG ZHANG², QIUYUE LI², XINYU LIU² and YU LI¹

¹Engineering Research Center of Chinese Ministry of Education for Edible and Medicinal Fungi, Jilin Agricultural University, Changchun, Jilin 130118; ²School of Life Sciences, Jilin University, Changchun, Jilin 130012; ³Zhuhai College of Jilin University, Jilin University, Zhuhai, Guangdong 519041, P.R. China

Received May 19, 2016; Accepted April 11, 2017

DOI: 10.3892/mmr.2017.6745

Abstract. The present study aimed to investigate the neuroprotective effect of a novel synthetic compound (5zou) on differentiated PC12 cells against 6-hydroxydopamine (6-OHDA) and L-glutamic acid (L-Glu) neurotoxin-induced cell injury and the potential mechanisms involved. 5zou is a 2, 2-disubstituted 1,2-dihydropyridine. PC12 cells were treated with 6-OHDA and L-Glu to establish neurotoxic cell models. MTT assay, DCFH-DA staining, Fluo-4-AM staining, JC-1 staining and western blotting were used to determine the changes in cell viability, intracellular reactive oxygen species concentration, Ca²⁺ influx, mitochondrial membrane potential and the protein expressions of B-cell lymphoma-2 (Bcl-2) and B-cell lymphoma-extra large (Bcl-xL). Morphological analysis demonstrated the effect of 5zous on neuritogenesis and differentiation in PC12 cells. The results suggested that 5zou rescued the cell viability, intracellular ROS level, Ca²⁺ influx, mitochondrial membrane potential, and expression of Bcl-2 and Bcl-xL, which were altered by 6-OHDA and L-Glu. The study confirmed that 5zou has neuroprotective effects on neurotoxin-induced differentiated PC12 cells injury, potentially via the mitochondrial apoptosis pathway.

Introduction

Neurodegenerative diseases are caused by chronic progressive degenerative damage of the central nervous system (1). The number of individuals suffering from neurodegenerative diseases is growing (2). Although the apoptotic cells in brain

area have been observed in patients with Parkinson's and/or Alzheimer's disease, the pathogenic mechanism is not clearly established yet (3). Recent studies demonstrate that the regulation of apoptosis has become a target for prevention and treatment in neurodegenerative diseases (4,5).

Various signals are involved in the apoptotic process. As a second messenger, intracellular calcium is required at low level to maintain homeostasis; however, calcium overload produces large amounts of reactive oxygen species (ROS), which interferes with the electron transport chain and reduces the formation of ATP (6). High levels of calcium and ROS promote the opening of mitochondrial permeability transition pores, which leads to mitochondrial membrane potential dissipation (7). Mitochondrial energy dysfunction will lead to apoptosis (8). Anti-apoptotic proteins B-cell lymphoma-2 (Bcl-2) and B-cell lymphoma-extra large (Bcl-xL) are highly concentrated in the outer membrane of mitochondria and are responsible for mitochondria-mediated apoptosis (9).

SH-SY5Y human neuroblastoma cells and PC12 rat pheochromocytoma cells are common cell models for *in vitro* investigation of neurodegenerative diseases. PC12 cells have obvious synapses formation, and are capable of producing nerve-related proteins following stimulation by nerve growth factor (NGF) (10). Certain small synthetic molecules have been reported to exhibit neuroprotective activities against neurotoxin-induced toxicity in SH-SY5Y and PC12 cells via mitochondrial pathways (11,12).

The present study examined the neuroprotective effect of a series of 2,2-disubstituted derivatives in differentiated PC12 (DPC12) cells (Table I). Following morphological screening, one synthetic small molecule (5zou) exhibited significant protection against 6-hydroxydopamine (6-OHDA) and L-glutamic acid (L-Glu)-induced cell damage. The molecular mechanisms associated with mitochondria were investigated further.

Materials and methods

Synthesis of compound 5zou. Under an N₂ atmosphere at 30°C were added 1,4-diazabicyclo [2.2.2] octane (20 mol%), compound 1 (as presented in Fig. 1; 1 mmol, 291 mg), MBH carbonate (1.2 mmol, 276 mg) and CH₃CN (10 ml) to a dried 10 ml reaction tube. The reaction was monitored by thin layer

Correspondence to: Professor Yu Li, Engineering Research Center of Chinese Ministry of Education for Edible and Medicinal Fungi, Jilin Agricultural University, 2888 Xincheng Street, Changchun, Jilin 130118, P.R. China
E-mail: yuli966@126.com

*Contributed equally

Key words: neuroprotection, 6-hydroxydopamine, L-glutamate, mitochondria, synthesis

chromatography (TLC). Upon completion, the reaction mixture was concentrated *in vacuo*. The crude mixture was purified by column chromatography [silica gel, EtOAc/petroleum ether (60–90°C)] to provide compound 3 (299 mg, 77% yield). mp: 78.5–79.2°C; ¹H NMR (300 MHz, CDCl₃) δ 7.23 (d, J=0.9 Hz, 1H), 6.36 (d, J=0.9 Hz, 1H), 6.13 (dd, J=9.8, 0.9 Hz, 1H), 5.72 (s, 1H), 5.43 (dd, J=9.8, 0.8 Hz, 1H), 4.41 (q, J=7.1 Hz, 2H), 3.72 (s, 3H), 3.70–3.65 (m, 4H), 3.61 (d, J=13.9 Hz, 1H), 3.55–3.50 (m, 4H), 2.83 (d, J=13.8 Hz, 1H), 1.41 (t, J=7.1 Hz, 3H). ¹³C NMR (125 MHz, CDCl₃) δ 167.08, 166.92, 152.20, 132.95, 131.96, 130.26, 122.82, 118.35, 117.42, 109.65, 66.90, 64.55, 57.37, 52.42, 45.61, 40.33, 14.33. HRMS (ESI): calcd. for C₁₉H₂₄N₃O₆ ([M+H]⁺): 390.1660, found 390.1650 (13).

Cell culture. PC12 rat adrenal cells (obtained from the American Type Culture Collection, Manassas, VA, USA; CRL-1721; passages <10) were cultured in Dulbecco's modified Eagle medium (DMEM; Invitrogen; Thermo Fisher Scientific, Inc., Waltham, MA, USA) which was supplemented with 5% horse serum (Invitrogen; Thermo Fisher Scientific, Inc.), 10% fetal bovine serum (FBS; Invitrogen; Thermo Fisher Scientific, Inc.), penicillin (100 U/ml), and streptomycin (100 µg/ml) (Invitrogen; Thermo Fisher Scientific, Inc.), under a humidified atmosphere containing 5% CO₂ at 37°C. The culture medium was changed every three days. PC12 cells were differentiated for 48 h using 50 ng/ml of NGF (Sigma-Aldrich; Merck KGaA, Darmstadt, Germany) dissolved in DMEM medium containing 1% FBS, 1% horse serum and 100 U/ml penicillin/streptomycin.

Cellular morphology analysis. PC12 cells were seeded in 6-well plates at 2 × 10⁴ cells/well. After replacing the medium with serum-free basic medium, cells were treated with 40 µM of the synthetic compounds detailed in Table I, and 10, 20 and 40 µM 5zou for 24 h and then imaged using an inverted microscope (x10; Nikon Corporation, Tokyo, Japan). Cells with projections and a longer neurite (neurite length range, 5–37 µm), compared with untreated undifferentiated cells (neurite length range, 2–15 µm), were considered as differentiated.

Cell viability analysis. DPC12 cells were seeded in 96-well plates at 2 × 10⁴ cells/well, and pretreated with 5zou (10–40 µM) for 3 h, and then exposed to 100 µM 6-OHDA and 25 mM L-Glu for another 24 h. After incubation with MTT solution (0.5 mg/ml) for 4 h at 37°C in darkness, 100 µl dimethyl sulfoxide was added to dissolve crystals. A microplate reader (Bio-Rad Laboratories, Inc., Hercules, CA, USA) was used to measure the absorbance at 540 nm. Viability values were expressed as a percentage of that of corresponding control cells.

Hoechst staining analysis. Nuclear morphological alterations were analyzed by Hoechst 33342 staining. DPC12 cells were pre-treated with 20 and 40 mM 5zou for 3 h, followed with 24 h co-incubation with 100 µM 6-OHDA and 25 mM L-Glu. Then cells were incubated with Hoechst 33342 (5 µg/ml; Sigma-Aldrich; Merck KGaA) for 15 min at 37°C in darkness. After washing with PBS, the fluorescence intensity in the nucleus was captured using a fluorescent microscope (x20; Axio Observer Z1; Carl Zeiss AG, Oberkochen, Germany).

The percentage of damaged cells was analyzed by measuring the blue fluorescence intensity using Image J 1.38x software (National Institutes of Health, Bethesda, MA USA).

Intracellular calcium concentration ([Ca²⁺]_i) analysis. DPC12 cells were seeded in a 6-well plate (2 × 10⁵ cells/well). The next day, cells were treated with 20 and 40 µM 5zou for 3 h prior to co-incubation with 100 µM 6-OHDA and 25 mM L-Glu for 12 h. Then, the supernatant was removed, and cells were incubated with 5 µM Fluo-4-AM (Invitrogen; Thermo Fisher Scientific, Inc.) for 30 min at 37°C in darkness. After three washes, cells were observed using a fluorescence microscope (x20; Axio Observer Z1). The average of green fluorescence intensity was detected using Image J software and expressed as a percentage of that of the corresponding control cells.

Mitochondrial membrane potential (MMP) analysis. DPC12 cells (1 × 10⁵ cells/well) were seeded into a 6-well plate. Cells were pre-treated with 20 and 40 µM 5zou for 3 h, followed with 12 h co-incubation with 100 µM 6-OHDA and 25 mM L-Glu. Treated cells were incubated with 2 µM 5,5',6,6'-tetrachloro-1,1',3,3'-tetraethyl-benzimidazolylcarbocyanine iodide (JC-1) (Sigma-Aldrich; Merck KGaA) at 37°C for 10 min. Fluorescent microscope (x20; CCD camera, Axio Observer Z1; Carl Zeiss, Germany) was applied to record the fluorescent color in each group. The ratio of red to green fluorescence intensity was detected by Image J software and expressed as a percentage of that of corresponding control cells.

Measurement of ROS. Intracellular ROS levels were analyzed using a ROS assay kit obtained from Nanjing Jiancheng Bioengineering Institute (Nanjing, China). DPC12 cells were exposed to 20 and 40 µM 5zou for 3 h, and co-incubated with 6-OHDA (100 µM) and L-Glu (25 mM) for 12 h. Treated cells were incubated with 10 µM dichlorofluorescein diacetate (DCFH-DA) at 37°C for 30 min. The fluorescent color was photographed by a fluorescent microscope (x20; Axio Observer Z1). The average green fluorescence intensity was detected by Image J and expressed as a percentage of that of corresponding control cells.

Western blot. DPC12 cells were pre-treated with 20 and 40 µM 5zou for 3 h, and followed with 24-h incubation of 6-OHDA (100 µM) and L-Glu (25 mM). Cells were lysed by radioimmunoprecipitation assay buffer (Sigma-Aldrich; Merck KGaA) containing 2% phenylmethanesulfonyl fluoride (Sigma-Aldrich; Merck KGaA) and 1% protease inhibitor cocktail (Sigma-Aldrich; Merck KGaA). Protein concentrations were determined using a Standard BCA Protein Assay kit (Merck KGaA). Proteins (30 µg) were separated on a 12% SDS-PAGE gel and electrophoretically transferred onto nitrocellulose membranes (Bio Basic, Inc., Markham, ON, Canada). The membranes were blocked in 5% bovine serum albumin at room temperature for 4 h, and then incubated with the following primary antibodies (all diluted 1:1,000) overnight at 4°C: Bcl-2 (ab321224), Bcl-xL (ab7973), and GAPDH (ab8245) (1:1,000; Abcam, Cambridge, UK) at 4°C overnight, followed by incubation with appropriate horseradish peroxidase-conjugated secondary

Table I. Neuroprotection screening of zou compounds.

Compound	R group	Differentiation status
1	CON(<i>i</i> Pr) ₂	N
2	CONEt ₂	N
3	CON(OMe)Me	N
4	CON(CH ₂) ₅	N
5	CON(CH ₂) ₄ O	Y
6	CO ₂ Me	N
7	CN	N

Differentiation status was determined by morphological analysis. PC12 cells were treated with each compound (40 μ M) for 24 h and subsequently imaged using an inverted microscope.

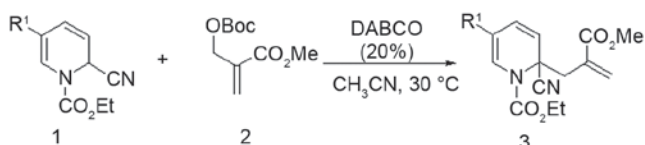


Figure 1. Procedure for novel zou (compound 3) preparation.

antibodies (sc-2005 and sc-358925) at dilution of 1:2,000 at 4°C for 4 h (Santa Cruz Biotechnology, Inc., Dallas, TX, USA). Chemiluminescence was detected by using enhanced chemiluminescence detection kits (GE Healthcare Life Sciences, Little Chalfont, UK).

Statistical analysis. All data are presented as the mean \pm standard deviation. Data were evaluated by one-way analysis of variance to detect statistical significance, followed by post-hoc multiple comparisons (Dunn's test) using SPSS 16.0 software (SPSS Inc., Chicago, IL, USA). $P < 0.05$ was considered to indicate a statistically significant difference.

Results

5zou increases DPC12 cells differentiation. PC12 cells in the control group, treated with basic DMEM, were round, short spindle and triangular, and their nuclei were large and round. Cells became a polygonal shaped following 5zou treatment. With the increasing 5zou concentration, cell differentiation rate was increased (Fig. 2).

5zou protected neurotoxin-induced DPC12 cell damage. 6-OHDA and L-Glu resulted in a 60.8 and 57.2% reduction in cell viability, respectively ($P < 0.001$; Fig. 3), which was partially restored following 5zou pre-treatment ($P < 0.05$; Fig. 3).

Hoechst 33342 staining demonstrated that the nuclei in control cells exhibit a uniform weak light blue fluorescence. However, in 6-OHDA and L-Glu-treated DPC12 cells, most cells were asymmetrical and appeared chunky in shape with

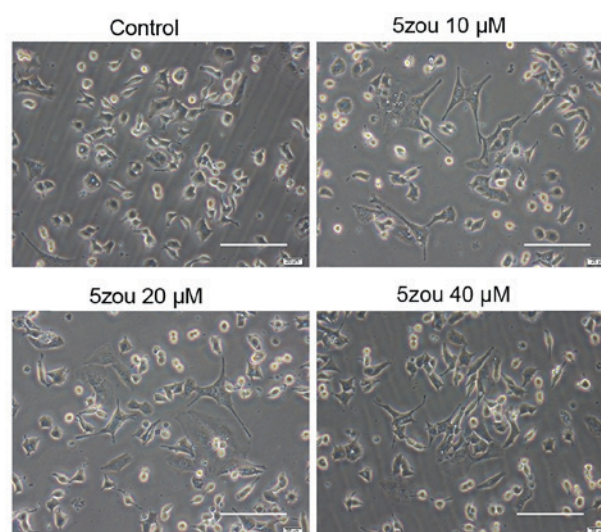
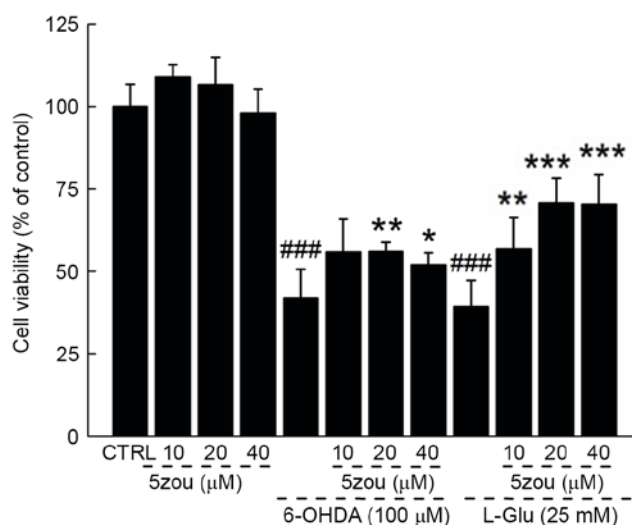
Figure 2. 5zou induced PC12 cell differentiation. Scale bar, 50 μ m.

Figure 3. 5zou increases the cell viability in differentiated PC12 cells exposed to 6-OHDA or L-Glu for 24 h. Data are expressed as the mean \pm standard deviation (n=6). ### $P < 0.001$ vs. CTRL; * $P < 0.05$, ** $P < 0.01$ and *** $P < 0.001$ vs. L-Glu-treated or 6-OHDA-treated cells. CTRL, control; 6-OHDA, 6-hydroxydopamine; L-Glu, L-glutamic acid.

intense blue fluorescence. Pretreatment with 5zou for 3 h pretreatment strongly reversed the nuclear damage in DPC12 cells ($P < 0.05$; Fig. 4).

Effects of 5zou on intracellular Ca²⁺ concentration, ROS levels and mitochondrial function. 6-OHDA and L-Glu increased the levels of intracellular Ca²⁺ in DPC12 cells after 12 h incubation (Fig. 5). Compared with model cells, 5zou reduced intracellular Ca²⁺ concentration, indicated by reduced green fluorescence ($P < 0.05$; Fig. 5).

DCFH-DA is oxidized to produce a highly fluorescent substance when oxidized, and is this used as a probe for measuring the levels of ROS. High green fluorescence was clearly observed in DPC12 cells treated with 6-OHDA and L-Glu, which was significantly reduced in 5zou-treated cells,

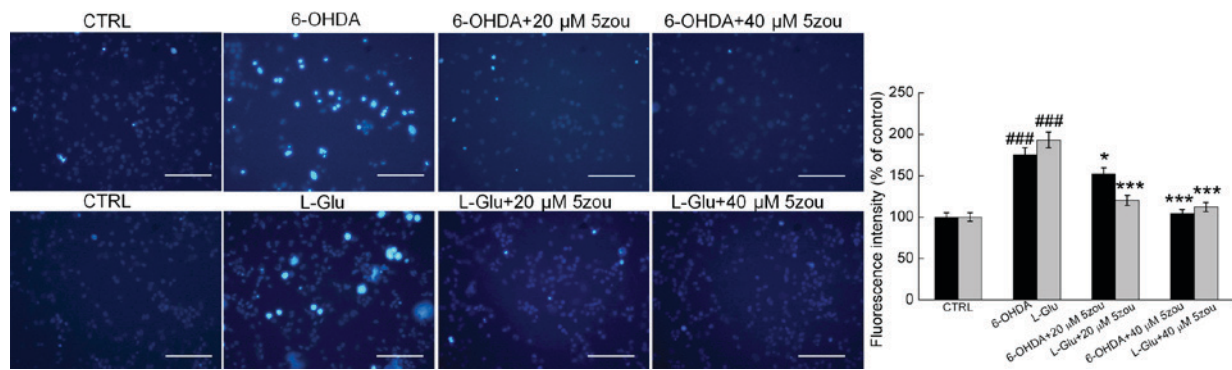


Figure 4. 5zou restored 6-OHDA or L-Glu-induced nucleus morphological alterations detected by Hoechst 33342 staining. Scale bar, 100 μm . Numerical data demonstrate the average blue fluorescence intensity. Data are expressed as the mean \pm standard deviation ($n=3$). ### $P<0.001$ vs. CTRL; * $P<0.05$ and *** $P<0.001$ vs. L-Glu-exposed or 6-OHDA-exposed cells. CTRL, control; 6-OHDA, 6-hydroxydopamine; L-Glu, L-glutamic acid.

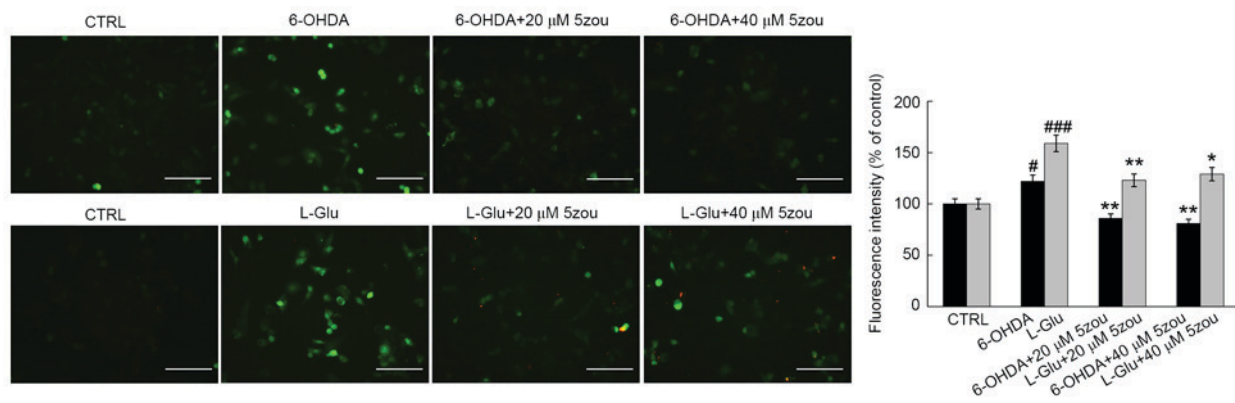


Figure 5. Intracellular Ca^{2+} overload induced by 6-OHDA or L-Glu is rescued by 5zou. Cells were stained with Fluo-4-AM. Scale bar, 100 μm . Numerical data demonstrate the average fluorescence intensity. Data are expressed as the mean \pm standard deviation ($n=3$). # $P<0.05$ and ### $P<0.001$ vs. CTRL; * $P<0.05$ and ** $P<0.01$ vs. L-Glu-treated or 6-OHDA-treated cells. CTRL, control; 6-OHDA, 6-hydroxydopamine; L-Glu, L-glutamic acid.

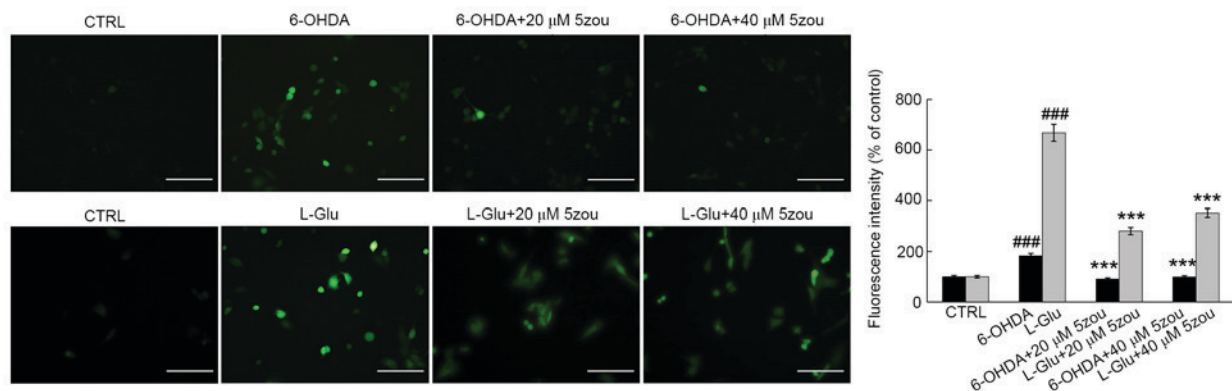


Figure 6. 5zou reduces accumulation of reactive oxygen species induced by 6-OHDA or L-Glu in differentiated PC12 cells. Cells were stained with dichlorofluorescein diacetate. Scale bar, 100 μm ($n=3$). Numerical data demonstrate by the average green fluorescence density. Data are expressed as the mean \pm standard deviation ($n=3$). ### $P<0.001$ vs. CTRL; *** $P<0.001$ vs. L-Glu-treated or 6-OHDA-treated cells. CTRL, control; 6-OHDA, 6-hydroxydopamine; L-Glu, L-glutamic acid.

suggesting 5zou successfully inhibited ROS accumulation ($P<0.05$; Fig. 6).

JC-1 staining is widely used as an indicator of the MMP, producing red fluorescence in normal cells and green fluorescence in unhealthy cells. In L-Glu and 6-OHDA treated cells, weak red fluorescence and strong green fluorescence were observed ($P<0.001$; Fig. 7). 5zou alleviated MMP dissipation

in neurotoxin-induced PC12 cells, indicated by the enhancement of red fluorescence ($P<0.001$; Fig. 7).

Effects of 5zou on Bcl-2 and Bcl-xL expression in PC12 cells. Compared with the control group, the protein expressions levels of Bcl-xL and Bcl-2 protein were decreased in PC12 cells treated with 6-OHDA and L-Glu

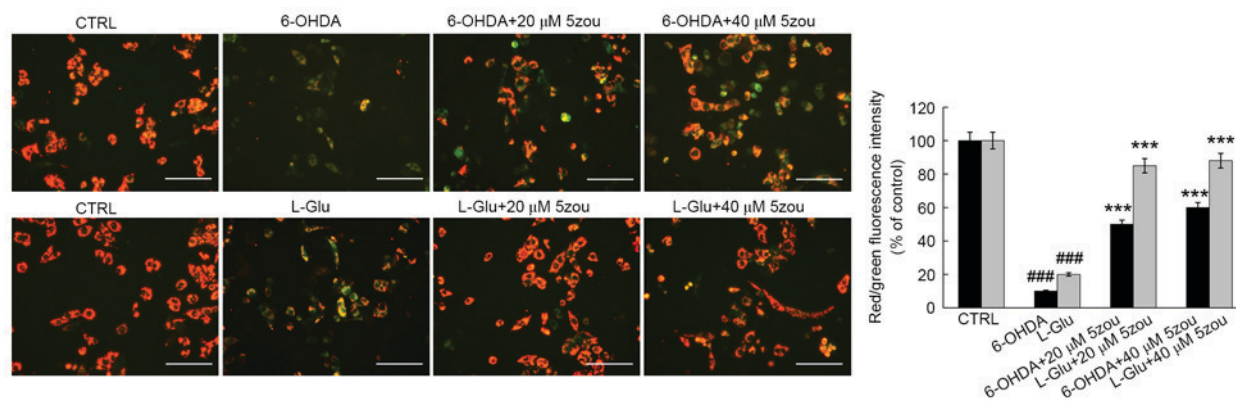


Figure 7. 5zou rescues the mitochondrial membrane potential disruption induced by 6-OHDA or L-Glu. Scale bar, 100 μm . Cells were stained with JC-1. Numerical data present the ratio of red to green fluorescence intensity. Data are expressed as the mean \pm standard deviation (n=3). ***P<0.001 vs. CTRL; **P<0.001 vs. L-Glu-exposed or 6-OHDA-treated cells. CTRL, control; 6-OHDA, 6-hydroxydopamine; L-Glu, L-glutamic acid.

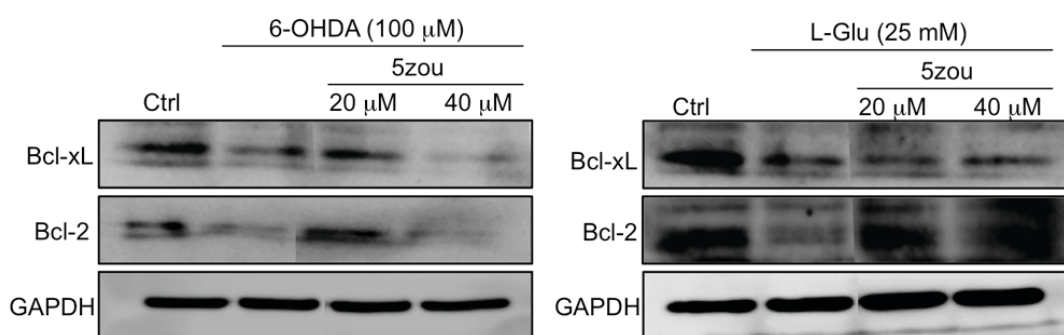


Figure 8. 5zou enhances Bcl-2 and Bcl-xL expressions in differentiated PC12 cells exposed to 6-OHDA and L-Glu for 24 h. Ctrl, control; 6-OHDA, 6-hydroxydopamine; L-Glu, L-glutamic acid; Bcl-2, B-cell lymphoma-2; Bcl-xL, B-cell lymphoma-extra large.

compared with control cells (Fig. 8). Pretreatment with 5zou, especially at 20 μM , increased the levels of Bcl-2 and Bcl-xL compared with 6-OHDA and L-Glu treatments. However, 40 μM 5zou failed to reverse the low expression levels of Bcl-xL and Bcl-2 in 6-OHDA-treated cells (Fig. 8).

Discussion

As the most important excitatory neurotransmitter in the central nervous system, glutamic acid has important roles in the formation of synapses. However, markedly increased glutamate levels, caused by physical or chemical factors, leads to excitatory neurotoxicity (14). 6-OHDA, a catecholamine hydroxylated derivative, is commonly used as a selective catecholaminergic nerve agent (15). In the present study, 6-OHDA and L-Glu were used to induce PC12 cell damage, and the protective effect of 5zou on cell apoptosis and the associated molecular mechanisms were subsequently examined.

In the present study, 5zou was been demonstrated to have a significant protective effect on 6-OHDA and L-Glu-induced cell viability reduction, Ca^{2+} overload, ROS accumulation and MMP dissipation. Mitochondria are the main organelle involved in cell energy metabolism. Intracellular Ca^{2+} overload is one of the main causes of mitochondrial dysfunction (16). Mitochondrial permeability is associated with cell toxicity, oxidative damage and apoptosis. The leakage from the mitochondrial respiratory

chain produces superoxide radicals, then causes ROS generation, which will ultimately lead to intracellular oxidative stress (17). ROS accumulation may further induce mitochondrial damage, which affects the respiratory chain and the inner and outer mitochondrial membrane proteins, resulting in cytochrome C release, and triggering of the mitochondrial apoptosis pathway (18). The imbalance of intracellular ROS homeostasis is considered to be responsible for cell oxidative damage (19). The data of the present study demonstrated that 5zou exhibited strong protective effects against neurotoxin-induced PC12 cell damage associated with ROS-dependent mitochondrial apoptosis.

Previous studies have demonstrated that the balance of Bcl-2 family members regulates mitochondrial function. 6-OHDA and L-Glu induce mitochondrial dysfunction by regulating the Bcl-2/Bax ratio in SH-SY5Y or PC12 cells, thus contributing to cell apoptosis (20,21). Bcl-2 suppresses apoptosis via two distinct pathways. The BH1-3 domains of Bcl-2 form a hydrophobic pocket, binding and inhibiting pro-apoptotic proteins, and additionally, inositol 1,4,5-trisphosphate receptors prevent Ca^{2+} influx-induced apoptosis (22). 5zou was demonstrated to improve the neurotoxin-induced MMP dissipation, and also inhibit the abnormal changes to Bcl-2 and Bcl-xL expressions. Thus, 5zou affects the mitochondrial apoptosis pathway to inhibit 6-OHDA and L-Glu-induced cell damage.

A high concentration of L-Glu was used in the present study. For *in vitro* experiments, 20-25 mM of L-Glu has been

previously used to induce damage of DPC12 cells (23,24). In previous experiments performed by our group, 25 mM L-Glu was used to establish neurotoxic DPC12 cell models (25). In the present study, fluorescence intensity measurements were normalized by cell counting of stained and unstained cells, which is a potential limitation; future studies will involve counterstaining, to further improve the accuracy of the results.

Notably, the results indicated that the same concentration of 5zou exhibited different effects on 6-OHDA and L-Glu damaged PC12 cells, which may be related to different injuries on the neurons, occurring via different signaling pathways. In conclusion, the present study demonstrated the neuroprotective effect of a novel compound (5zou). The effect of 5zou may be associated with the mitochondrial apoptotic pathway.

Acknowledgements

This work was supported by the Natural Science Foundation of China (grant no. 81402955), China's Post-doctoral Science Foundation (grant no. 2016M591495) and Post-doctoral Science Research Project in Jilin Province of China. Authors thank Professor Weiwei Liao (Department of Organic Chemistry, Jilin University, Changchun, China) for providing the 2,2-disubstituted derivatives.

References

- Amor S, Puentes F, Baker D and van der Valk P: Inflammation in neurodegenerative diseases. *Immunology* 129: 154-169, 2010.
- Head E: Combining an antioxidant-fortified diet with behavioral enrichment leads to cognitive improvement and reduced brain pathology in aging canines: Strategies for healthy aging. *Ann N Y Acad Sci* 1114: 398-406, 2007.
- Hurny A, Michalowska-Wender G and Wender M: Impact of L-DOPA treatment of patients with Parkinson's disease on mononuclear subsets and phagocytosis in the peripheral blood. *Folia Neuropathol* 51: 127-131, 2013.
- Balez R, Steiner N, Engel M, Muñoz SS, Lum JS, Wu Y, Wang D, Valloton P, Sachdev P, O'Connor M, *et al.*: Neuroprotective effects of apigenin against inflammation, neuronal excitability and apoptosis in an induced pluripotent stem cell model of Alzheimer's disease. *Sci Rep* 6: 31450, 2016.
- Zhang J, An S, Hu W, Teng M, Wang X, Qu Y, Liu Y, Yuan Y and Wang D: The neuroprotective properties of hericium erinaceus in glutamate-damaged differentiated PC12 Cells and an alzheimer's disease mouse model. *Int J Mol Sci* 17: pii: E1810, 2016.
- Murphy E and Steenbergen C: Mechanisms underlying acute protection from cardiac ischemia-reperfusion injury. *Physiol Rev* 88: 581-609, 2008.
- Akopova OV, Kolchynskaya LY, Nosar VY, Smyrnov AN, Malisheva MK, Man'kovskaia YN and Sahach VF: The effect of permeability transition pore opening on reactive oxygen species production in rat brain mitochondria. *Ukr Biokhim Zh* (1999) 83: 46-55, 2011.
- Liu CY, Lee CF and Wei YH: Role of reactive oxygen species-elicited apoptosis in the pathophysiology of mitochondrial and neurodegenerative diseases associated with mitochondrial DNA mutations. *J Formos Med Assoc* 108: 599-611, 2009.
- Oh KJ, Lee SC, Choi HJ, Oh DY, Kim SC, Min do S, Kim JM, Lee KS and Han JS: Role of phospholipase D2 in anti-apoptotic signaling through increased expressions of Bcl-2 and Bcl-xL. *J Cell Biochem* 101: 1409-1422, 2007.
- Su WT and Shih YA: Nanofiber containing carbon nanotubes enhanced PC12 cell proliferation and neuritegenesis by electrical stimulation. *Biomed Mater Eng* 26 (Suppl 1): S189-S195, 2015.
- Jackson TC, Verrier JD and Kochanek PM: Anthraquinone-2-sulfonic acid (AQ2S) is a novel neurotherapeutic agent. *Cell Death Dis* 4: e451, 2013.
- Kim IS, Koppula S, Kim BW, Song MD, Jung JY, Lee G, Lee HS and Choi DK: A novel synthetic compound PHID (8-Phenyl-6a, 7, 8, 9, 9a, 10-hexahydro-6H-isoindolo [5, 6-g] quinoxaline-7, 9-dione) protects SH-SY5Y cells against MPP(+)-induced cytotoxicity through inhibition of reactive oxygen species generation and JNK signaling. *Eur J Pharmacol* 650: 48-57, 2011.
- Zou GF, Hu ZP, Zhang SQ and Liao WW: Synthesis of functionalized 1,2-dihydropyridines bearing quaternary carbon centers via an organocatalytic allylic alkylation. *Tetrahedron Lett* 56: 937-940, 2015.
- Shimmyo Y, Kihara T, Akaike A, Niidome T and Sugimoto H: Three distinct neuroprotective functions of myricetin against glutamate-induced neuronal cell death: Involvement of direct inhibition of caspase-3. *J Neurosci Res* 86: 1836-1845, 2008.
- Yong Y, Ding H, Fan Z, Luo J and Ke ZJ: Lithium fails to protect dopaminergic neurons in the 6-OHDA model of Parkinson's disease. *Neurochem Res* 36: 367-374, 2011.
- Garcia-Rivas GJ and Torre-Amione G: Abnormal mitochondrial function during ischemia reperfusion provides targets for pharmacological therapy. *Methodist Debaque Cardiovasc J* 5: 2-7, 2009.
- Poyton RO, Ball KA and Castello PR: Mitochondrial generation of free radicals and hypoxic signaling. *Trends Endocrinol Metab* 20: 332-340, 2009.
- Kinnally KW and Antonsson B: A tale of two mitochondrial channels, MAC and PTP, in apoptosis. *Apoptosis* 12: 857-868, 2007.
- Goitre L, Balzac F, Degani S, Degan P, Marchi S, Pinton P and Retta SF: KRIT1 regulates the homeostasis of intracellular reactive oxygen species. *PLoS One* 5: e11786, 2010.
- Pislar AH, Zidar N, Kikelj D and Kos J: Cathepsin X promotes 6-hydroxydopamine-induced apoptosis of PC12 and SH-SY5Y cells. *Neuropharmacology* 82: 121-131, 2014.
- Sun R, Wang K, Wu D, Li X and Ou Y: Protective effect of paeoniflorin against glutamate-induced neurotoxicity in PC12 cells via Bcl-2/Bax signal pathway. *Folia Neuropathol* 50: 270-276, 2012.
- Lavik AR, Zhong F, Chang MJ, Greenberg E, Choudhary Y, Smith MR, McColl KS, Pink J, Reu FJ, Matsuyama S and Distelhorst CW: A synthetic peptide targeting the BH4 domain of Bcl-2 induces apoptosis in multiple myeloma and follicular lymphoma cells alone or in combination with agents targeting the BH3-binding pocket of Bcl-2. *Oncotarget* 6: 27388-27402, 2015.
- Wang D, Tan QR and Zhang ZJ: Neuroprotective effects of paeoniflorin, but not the isomer albiflorin, are associated with the suppression of intracellular calcium and calcium/calmodulin protein kinase II in PC12 cells. *J Mol Neurosci* 51: 581-590, 2013.
- Li W, Cheong YK, Wang H, Ren G and Yang Z: Neuroprotective effects of etidronate and 2,3,3-trisphosphonate against glutamate-induced toxicity in PC12 cells. *Neurochem Res* 41: 844-854, 2016.
- Hu S, Wang D, Zhang J, Du M, Cheng Y, Liu Y, Zhang N, Wang D and Wu Y: Mitochondria related pathway is essential for polysaccharides purified from *Sparassis crispa* mediated neuro-protection against glutamate-induced toxicity in differentiated PC12 cells. *Int J Mol Sci* 17: pii: E133, 2016.